Antarctic Science 14 (2), 185–194 (2002) © Antarctic Science Ltd Printed in the United Kingdom

Analysis of acoustic dot echo signature over an Antarctic ice shelf: the possible remote sensing of Antarctic petrels

PHILIP S. ANDERSON

British Antarctic Survey, NERC, High Cross, Madingley Road, Cambridge CB3 0ET, UK
philip.s.anderson@bas.ac.uk

Abstract: Data from a monostatic acoustic radar operating at British Antarctic Survey's Halley station on a coastal Antarctic ice shelf show a band of small target echoes at an altitude of 700–1000 m during spring 1991. Statistical analysis of the echo signature show that the targets are spread more evenly in the horizontal than would be expected for a random signature, whilst the local distribution in the vertical is Gaussian. Similar echo signatures have been observed previously, and are attributed to birds, bats or insects: the Antarctic data are also consistent with bird targets, but the case is not proven. No birds have been observed directly, but at 700 m they would be barely visible to the naked eye. The nearest nesting area with suitably large numbers of birds (Antarctic petrels, *Thalassoica antarctica*) is a few hundred kilometres away. Estimates of velocity and target density imply that the Halley site would need to be specially favoured by the colony for their acoustic signature to be observed in such numbers, but such might be the case due to the presence of perennial coastal open water to the west of the station.

Received 19 November 2001, accepted 24 February 2002

Key words: Antarctic petrel, dot echo, ice shelf, nocturnal boundary layer, polynya, Sodar

Introduction

During 1991, British Antarctic Survey operated an acoustic radar (Sodar) at Halley station, (75°35'S, 026°34'W in 2001), situated on the Brunt Ice Shelf (Fig. 1). Sodars transmit a short audible pulse of sound vertically and record the strength of any echo return; the time between pulse transmission and echo reception gives the range to the target. Sound propagating through the atmosphere is scattered by inhomogeneities in acoustic refractive index, essentially variability in temperature and wind velocity, the scattering being strongest by features in the scattering medium of a similar length scale to that of the wavelength of the sound. The Sodar at Halley was deployed as part of a micro-meteorological programme studying waves and turbulence in the lower atmosphere; wind shear acting on a temperature gradient tends to produce turbulent mixing which is suitable for generating the appropriate refractive index variability that causes acoustic scattering. The system thereby gives a qualitative picture of the turbulence in the lower atmosphere.

The Sodar in question transmitted a loud acoustic pulse vertically every 10 s, and then recorded the strength of the echo at the same location. In this monostatic mode, the instrument is recording 180° backscatter; scattering is very weak, and the echo is completely inaudible. Echo profiles are usually displayed as adjacent grey scale lines, building into an echogram as seen in Fig. 2. Here, a few hours of typical data are presented, where the darkness of the image implies the strength of the echo return, adjusted for range attenuation.

Subsequent analysis of the data from 1991 showed layers of atypical echo return above 500 m, which on closer inspection appeared to be point-like or "dot echoes", unlike the more diffuse echoes nearer the ground. This feature was observed

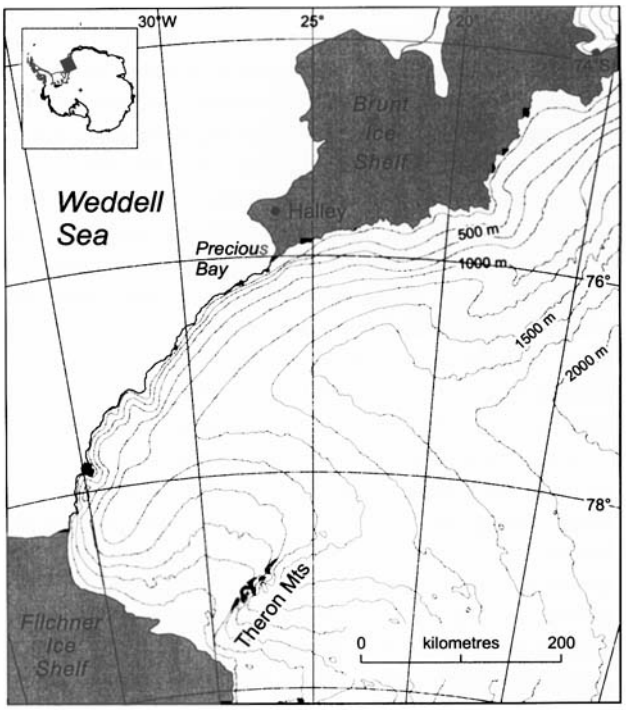

Fig. 1. Map of the Brunt Ice Shelf and local continental rise, indicating the position of Halley research station relative to the coast and the Theron Mountains. The bight to the south-west of the station is Precious Bay, an area of perennial open water.

https://doi.org/10.1017/S0954102002000755 Published online by Cambridge University Press

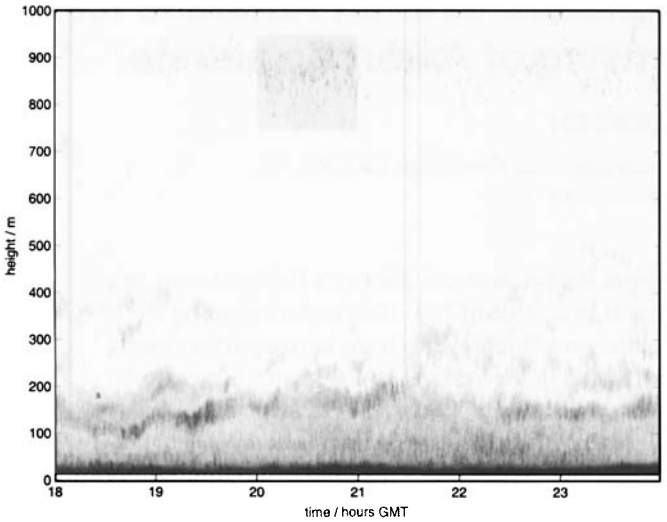

Fig. 2. Six hours of a typical Sodar echogram recorded at Halley on 30 September 1991; the vertical range is from the surface up to 1000 m. Atmospheric backscatter is evident as dark layers in the lower half of the image, whilst the dot echo signature appears as a band at around 900 m. The shadow area is shown in greater detail in Fig. 5.

in late winter and spring. Each dot would be limited in vertical extent and be comparatively strong compared to the more usual signature.

Similar data have been noted previously in both acoustic and radar atmospheric profilers, (Mastrantonio *et al.* 1999, Petenko & Kalistratova 1996) and have been identified with non-atmospheric effects such as bats, birds or insect swarms. The assumption that the dot echoes recorded at Halley are also of a biological origin must be tentative, as, at this time, there has not been significant bird activity seen over the station. A few bird species are observed directly in the vicinity of the base in summer, but always in small numbers: Antarctic skuas (*Catharacta maccormicki*), Arctic terns (*Sterna paradisaea*), Antarctic petrels (*Thalassoica antartica*) and snow petrels (*Pagodroma nivea*), have been seen at the Brunt Ice Shelf coast, with the occasional single bird or pair visiting the base for a short period. The ice shelf itself offers no nesting sites for such birds, and the species seen were assumed to be in transit.

Aside from flightless emperor penguins (*Aptenodytes forsteri*), all Antarctic bird species need rock to nest upon. Halley, being situated on an ice shelf, does not provide such a habitat. Similarly, the continental rise to the south of the station is completely ice covered for 350 km, until the Theron Mountains (Fig. 1). Reports from field parties working in the Theron range identified large numbers (10 000 estimated pairs) of Antarctic petrels (*Thalassoica antarctica*) nesting on scree on a north facing rock balcony (Brook & Beck 1972), and a much smaller number of snow petrels (*Pagodroma nivea*) (Croxall *et al.* 1995). These numbers were later confirmed by B. Storey (personal communication 1999) who, during a geological survey of the range in 1998, was able to confirm opportunistically the nesting of Antarctic petrels on the broad ledges of the escarpment. In both reports, the nests were found to be densely packed, about one every square metre, such that each nest was just beyond inter-pecking distance, implying that suitable nest sites were at a premium. From the total area of similar rock surface on the escarpment, that is, of similar slope and free of snow, the number of possible nesting sites could have been up to 40 000. Dr Storey records that the air was full of birds in flight, too numerous to count, and this upper estimate was thought to be quite believable.

Although the existence of birds in the Theron Mountains has been shown, and these birds may well migrate towards the coast *via* Halley (why is discussed below), the identity of dot echo signature on the acoustic radar has yet to be proven. This paper presents a statistical analysis for the target signature, which implies that the targets are non-atmospheric. In addition, should their identity be later proven, the remote sensing data may be of some interest on the target behaviour aloft.

Methods

The acoustic backscatter time series were recorded by a single antenna non-Doppler monostatic acoustic radar (Sodar). The original system by Sensitron recorded echo strength to a facsimile style recorder. The effects of beam spreading with range is offset by ramped gain amplification within the Sodar control unit. Each pulse was of 30 ms duration, with a smoothed bell shaped waveform envelope, such that the bulk of the pulse power was contained within the inner 15 ms of the envelope, equivalent to a vertical pulse length of 5 m. Pulse frequency was 2.3 kHz through a tuned acoustic driver operating at 120 W. Pulse repetition was 10 s, ensuring no aliasing in the echo return from previous pulse transmission. The echo sampling frequency was equivalent of 2 m resolution.

The Sodar antenna was positioned to the south and east of Halley, away from local buildings and in an area with a surface highly representative of the undisturbed ice shelf. Halley itself is situated towards the seaward edge of the Brunt Ice Shelf, about 16 km inland from the coast to the north and 22 km from the coast to the west.

The antenna comprised the acoustic driver, a parabolic dish and an acoustic baffle. The driver faced downward at the focus of the dish, which had a diameter, D, of 0.90 m. For a sound pulse of frequency f = 2.3 kHz and speed c = 330 ms^{-1}, the acoustic wavelength, λ, is 0.143 m. The beam amplitude, A, as a function of off-axis or zenith angle, ω, is given by:

$$A(\omega) = \frac{J_1(\Delta \sin(\omega))}{\Delta \sin(\omega)} \quad (1)$$

where J_1 is the first order Bessel function, and $\Delta = \pi D/\lambda$ is the size parameter (S. Bradley, personal communication 2001). From equation 1 the half amplitude angle of the beam (3 dB point) is at an angle of 6.3° off axis, whilst the first null point,

https://doi.org/10.1017/S0954102002000755 Published online by Cambridge University Press

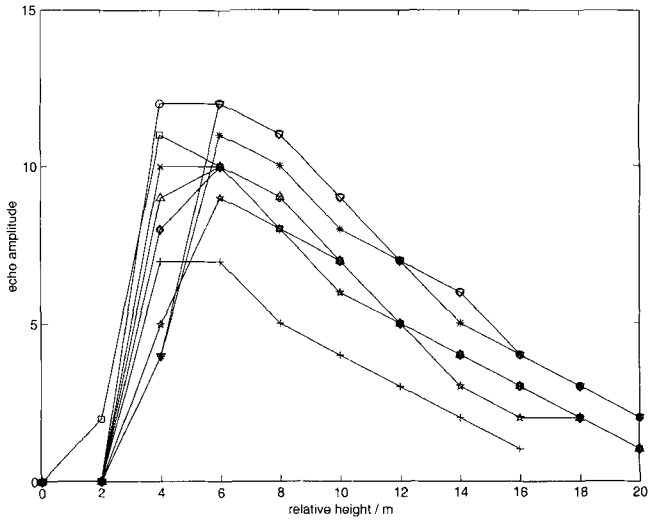

Fig. 3. A number of dot echo profiles overlaid with a common starting point, showing the similarity of the trailing slope irrespective of the amplitude of the peak.

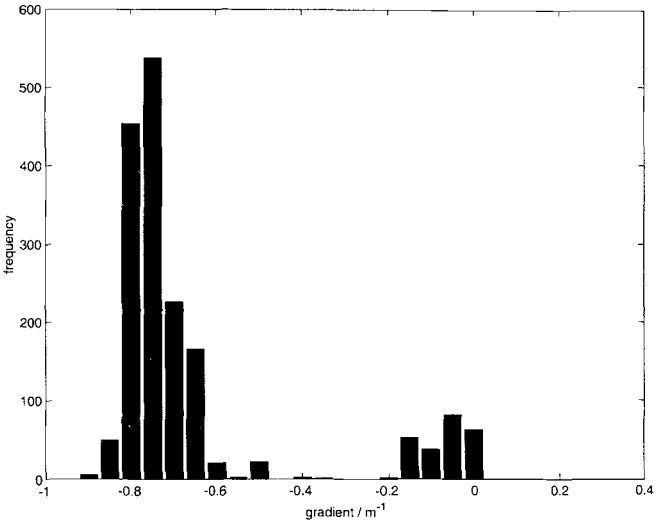

Fig. 4. Histogram of trail edge slope for all profile maxima for six hours of data. The dot echo slopes are grouped around 0.75 m^{-1} with a Gaussian distribution, allowing a quantitative detection of this echo type.

where the beam amplitude is zero, is at 11.2°. The antenna is baffled to absorb sound in the near-region for zenith angles greater than 9°. The horizontal cross sectional area of the beam as a function of range, z, is therefore given by:

$$C_3(z) = \pi\left(z\tan(6.3^o)\right)^2 = 0.0123z^2$$
$$C_{null}(z) = \pi\left(z\tan(11.2^o)\right)^2 = 0.0392z^2 \quad (2)$$

where C_3 is the area for the 3 dB angle, and C_{null} the area for the null angle. These will be taken as the experimental uncertainty in cross sectional area in the analysis below. For a vertical range of 700 m, this gives the beam sampling an area of between 6000 m^2 (0 to 3 dB) and 19 000 m^2 (all the main beam).

The backscatter output signal amplitude was digitised to 12 bit resolution and then compressed logarithmically from 12 bit to 4 bit (16 levels) resolution. Sodar echograms are generally presented as grey scale time/height images, where the darkness of the image implies strength of return echo. The duration from pulse transmission to the echo return, T_p, is represented as an effective height, z, using an estimate of the speed of sound in air, c, such that $z = c.T_p/2$.

Figure 2 is an example of a Sodar echogram from 18:00 GMT to 24:00 GMT for the 30th September 1991. Dot echoes are apparent between 700 and 1000 m altitude, along with a typical lower echo structure which is more diffuse and continuous in comparison. Figure 3 shows height/amplitude plots of a few typical dots overlaid, indicating that the general dot envelope has a sharp rise, followed by a linear sloping tail. The slope of the decay section is similar between dots, irrespective of the maximum amplitude of the envelope. This envelope shape may be explained by digitisation and a highly tuned receiver circuit: the digital sampling frequency of the backscatter envelope equates to a 2 m resolution, but the acoustic pulse duration of 15 ms equates to a spatial length of around 6 m. Hence a small reflector (< 2 m) would generate a pulse echo lasting at least 2–3 samples. However, the highly tuned filtering circuits within the Sodar receiver generate Gibbs phenomena, or ringing, which in turn produces an exponential decay in received power. In such a system, a perfect small reflector would generate an exponentially decaying signal but, because the digitised data is the logarithm of the backscatter power, the recorded decay is linear. The implication, though not proven, is that the "large" dots, apparently spreading over a few metres in the vertical, are in fact due to ringing generated by a strong echo return from a target which is, nonetheless, smaller than the pulse resolution.

The consistent nature of the Gibbs decay effect is confirmed in Fig. 4, a histogram of envelope decay slope for all local maxima detected in Fig. 2. The dot signature is readily apparent as the leftmost group of slope, centred on -0.75 m^{-1}. The detection algorithm is confirmed by comparing this method for non-dot records, where the slopes are clustered about -0.2 to 0. The exact values of these slopes are dependent upon the logarithmic compression algorithm and the electronic filtering, but the general technique should be universal. Given the form of the left hand distribution in Fig. 4, dots can be detected automatically as those peaks which fit this slope selection criteria. Figure 5 shows a magnified section of Fig. 2 with the positions of the detected dots overlaid as crosses. The dot detection method gives a quantitative time series of target heights, which in turn allows an assessment of the apparent randomness in the target distribution.

https://doi.org/10.1017/S0954102002000755 Published online by Cambridge University Press

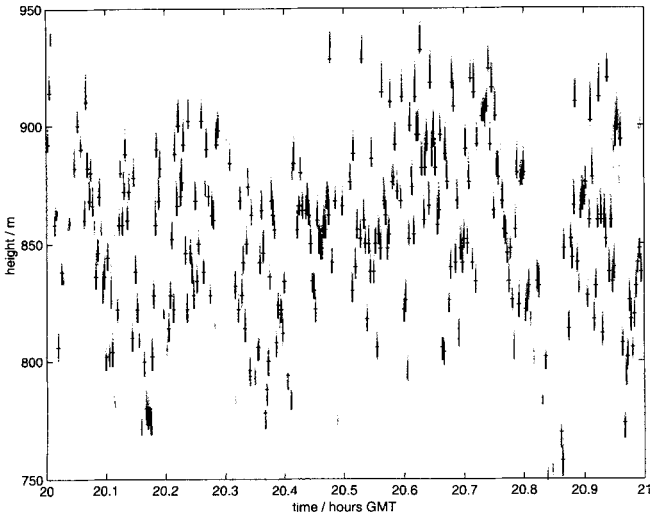

Fig. 5. Magnified section of Fig. 2 showing detail of the dot echo signature. Crosses indicate where the detection algorithm has found the lower limit of a dot.

Results

The Sodar operated continually from March through to November of 1991, except for periods when noise from high surface wind speeds (> 8 ms^{-1}) obliterated the acoustic signal. The echogramme images show the following general observations:

- Dots appear for the first time on 24 August.
- Dots are initially visible at the very top of the charts (1000 m altitude), but appear to exist above this height (see below)

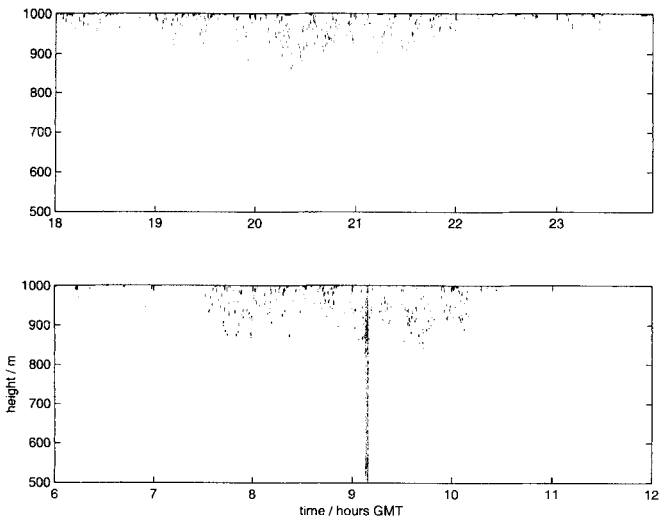

Fig. 6. Six-hour echogrammes for 12 and 25 October 1991, where the band of dots appears to rise above the altitude limit of the Sodar data, implying that on occasions when dots are not observed, they may still exist at heights just in excess of 1000 m.

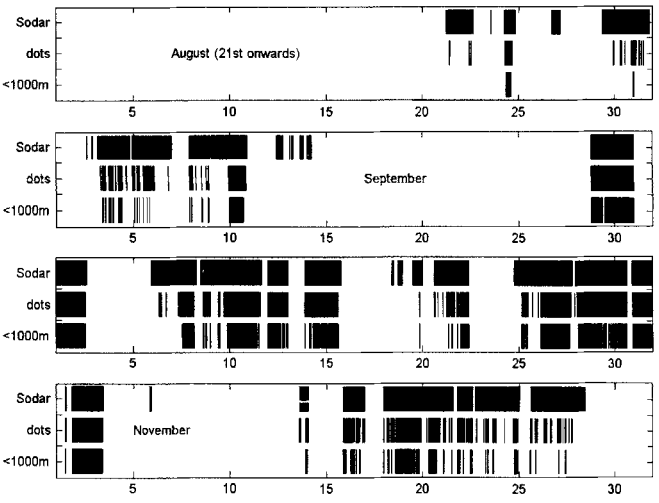

Fig. 7. Summary of the occurrence of dots during spring and autumn 1991. The total Sodar data coverage is indicated by the upper bar for the last four months of Sodar operation. Gaps in the Sodar data are due to wind noise. The occurrence of dot signature is given in the central bar, indicating the near continual dot signature when data were available. Dot signature clearly below the 1000 m Sodar data limit is given in the lower bar, defined as where the mean height is more than two standard deviations from the upper 1000 m bound. At the start of the observations, the dot band tended to be nearer this upper limit.

- The dots are limited to a band about 50–200 m deep.
- During the period of dot echo observation, the band of echo is seen at progressively lower levels at later dates.
- The last few records of Sodar operation (November)

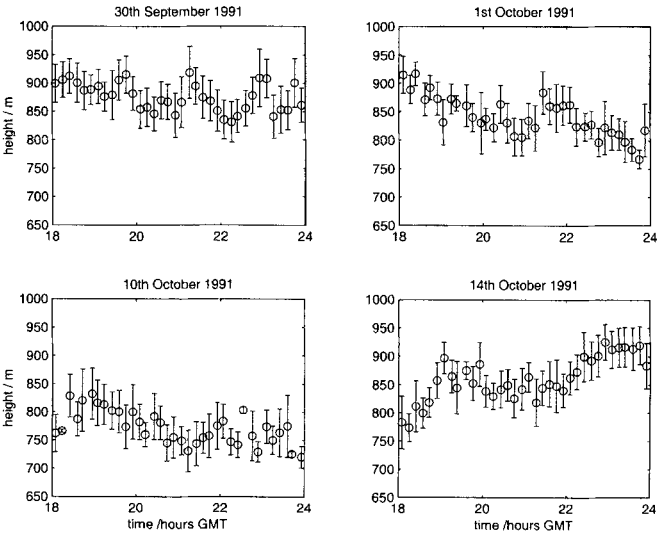

Fig. 8. 10 minute means and local vertical variance of the detected dot signature for four case study days. The vertical variance is similar over time, and between days, although the local height varies to some extent.

https://doi.org/10.1017/S0954102002000755 Published online by Cambridge University Press

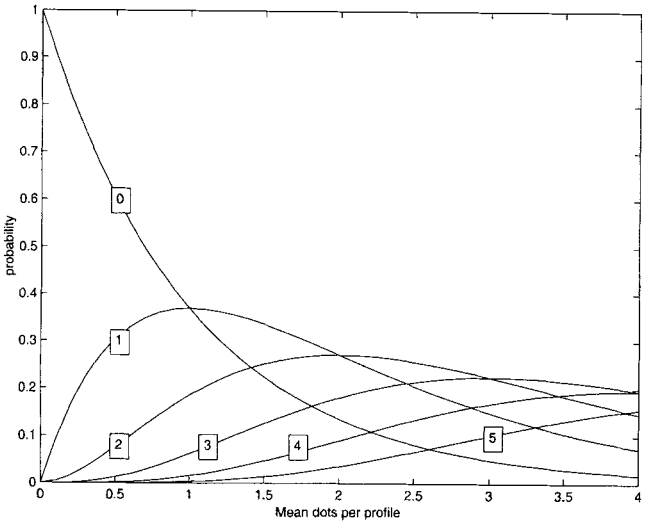

Fig. 9. Dependence of $P_r(x)$, the probability of x targets per profile, on the mean target density, d_{pp}, assuming a random distribution. Maximum $P_r(x) < 0.35$. The measured $P_d(1)$ of 0.7 implies that the dot signature are not randomly distributed in time.

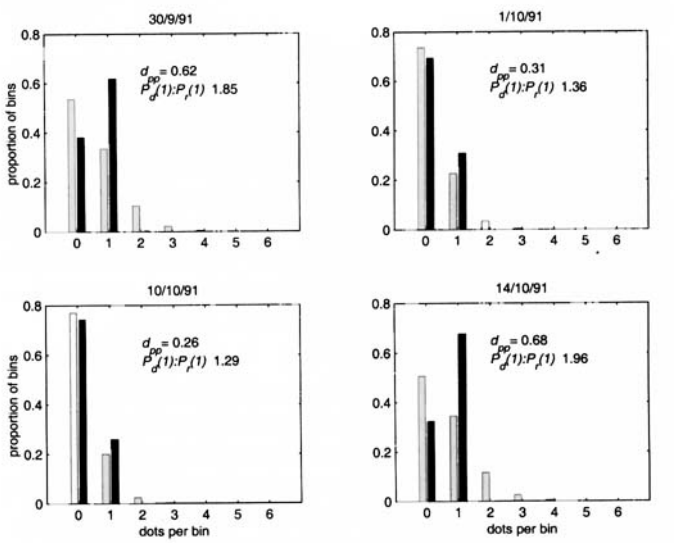

Fig. 10. Normalized distribution of the number of dots detected in each profile for the four study periods ($P_d(x)$, dark bars) compared to the expected distribution for a random scattering in time of the same density of targets ($P_r(x)$, light bars). The data show a marked increase in single dot profiles, with a corresponding decrease in all other bins.

shows some dot echo signature, but the signal is less distinct than in previous weeks.

The dot echoes signature is usually seen to be in a band that rises and falls over hours and days. Occasionally, the band rises towards the upper altitude limit of the Sodar data (1000 m), whereupon it disappears as if rising above the observation frame, and not as if it becomes extinguished; two examples of this effect are shown in Fig. 6. This implies, but does not prove, that a lack of observed dot echo signature is occasionally due to the targets being above 1000 m.

A summary of the occurrence of the dots is given in Fig. 7, which gives the dates and times of records where dots were observed, and where the band of dots was clearly below the upper 1000 m data limit, all compared to the overall Sodar data availability.

Four Sodar echogrammes of six hour duration were chosen for a more detailed analysis, and these contiguous series have been filtered as described above in order to retrieve a time series of mean target height. The data were selected for days when the observed dot echo band was well below the upper range of the Sodar (1000 m); height, and standard deviation of the four resulting time series are presented as error bar plots in Fig. 8. Table I presents the statistical analysis for the case studies, giving mean target height, $\langle z \rangle$, and the standard distribution, σz. The data were also re-sampled into 10 min bins, and the standard deviation, Fz_i of each bin calculated. This gives a measure of the 'local depth' or vertical spread of the dot echo layer at that time and is used to give the error bars in Fig. 8. The means of these local depths, $\langle \sigma z_i \rangle$ and the standard deviations, $\sigma(\sigma z_i)$ are also given in Table I.

Table I. Statistics for four periods when the dot signature is well within the Sodar range, shown as error bar plots in Fig. **8**. All data are for 18:00 GMT to 24:00 GMT.

Date	d_{pp}	$\langle z \rangle$/m	σz/m	$\langle \sigma z_i \rangle$/m	$\sigma(\sigma z_i)$/m
30/09/91	0.62	876	25.6	35.0	5.56
01/10/91	0.31	841	35.2	30.9	8.84
10/10/91	0.26	722	29.9	32.3	12.36
24/10/91	0.68	860	39.4	33.4	7.20

d_{pp} is mean number of dots per profile over the period. $\langle z \rangle$ and σz refer to the mean dot signature height and its variability over the six hour sampling period. $\langle \sigma z_i \rangle$ is the mean value of the 10 min standard deviations, whilst $\sigma(\sigma z_i)$ is the standard deviation of the set of σz_i. Essentially, $\langle \sigma z_i \rangle$ is the local mean depth of the dot band, with $\sigma(\sigma z_i)$ the uncertainty in $\langle \sigma z_i \rangle$.

Given a *random* distribution of m items (dots) in n bins (profiles), the probability $P_r(x)$ of a bin containing exactly x items is given by:

$$P_r(x) = \frac{m!}{(m-x)!\,x!} \cdot \frac{(n-1)^{m-x}}{n^m} \qquad (3)$$

This function is shown in Fig. 9 for the first few values of x, and as a function of $m/n = d_{pp}$. The set of values of $P_r(x)$ for a given d_{pp} are compared to the measured probability observed in the dot echo data, $P_d(x)$ in Fig. 10.

There is a noticeable difference in the empty and singleton bins, $P(0)$ and $P(1)$, as well as a less striking but equally significant difference in the higher order bins. The discrepancy is greatest for the higher density days, 30/9/91 and 24/10/91, where mean dot density, $\langle d_{pp} \rangle$, is 0.65, and $P_d(1):P_r(1)$ is 1.91, that is the data exhibit almost twice the number of single target profiles than would be expected from a random scattering. For the lower density days, 1/10/91 and 10/10/91, $\langle d_{pp} \rangle = 0.28$ and

https://doi.org/10.1017/S0954102002000755 Published online by Cambridge University Press

$P_d(1):P_r(1) = 1.32$.

For large m, in this case about 2000, and with d_{pp} of the order of unity, the expected sampling variance in each of the $P(x)$ values is less than 5%, and hence these differences between $P_r(x)$ and $P_d(x)$ are highly statistically significant. This difference is not due to miscounting as shown by the maximum in $P_r(1)$ in Fig. 9: this maximum is at around $d_{pp} = 1$, with a value of 0.35, whilst the data show a $P_d(1)$ of up to 0.7. These results are strong evidence that the distribution of the targets is not random, but maximises the mean separation.

$P_d(1)$ may be biased towards higher values by "persistence" in the targets, i.e. there are fewer actual targets, but they remain in the beam detection volume for more than one profile. This would lead to an over-counting of targets (enhance d_{pp}) as well as an over-counting of $P_d(1)$, as any (rare) genuine single target would generate a number of apparent single target profiles.

Two methods are used to check for this effect. Firstly by analysis of the distribution of singleton "runs", and secondly by the distribution of height difference between targets in adjacent profiles. A "singleton run" is an unbroken series of single target profiles. The expected distribution, $P(l)$, of runs of different length, l, is related to P_s, the probability of any given profile containing a target by:

$$P(l) = (1 - P_s)P_s^{(l-1)} \qquad (4)$$

This neglects multiple target profiles; P_s is therefore the total number of targets divided by the total number of profiles, that is $P_s = d_{pp}$. Figure 11 shows the distribution of singleton runs from the four six-hour periods presented above, alongside the expected distribution for the corresponding value of d_{pp}. The general agreement between data and expected frequency is good, indicating a negligible persistence in the target signature, and hence implying that the detected dots are, indeed, individual targets. The greatest discrepancy is shown on the last plot, 14 October, when there are apparently a greater than expected number of lone targets, that is, single target profile with no observed targets in the previous or following profile. That these data are for the day with the highest d_{pp} support the case that the target distribution is smoother in time than expected, as at these densities, the number of such lone targets expected from a random scattering becomes significantly reduced.

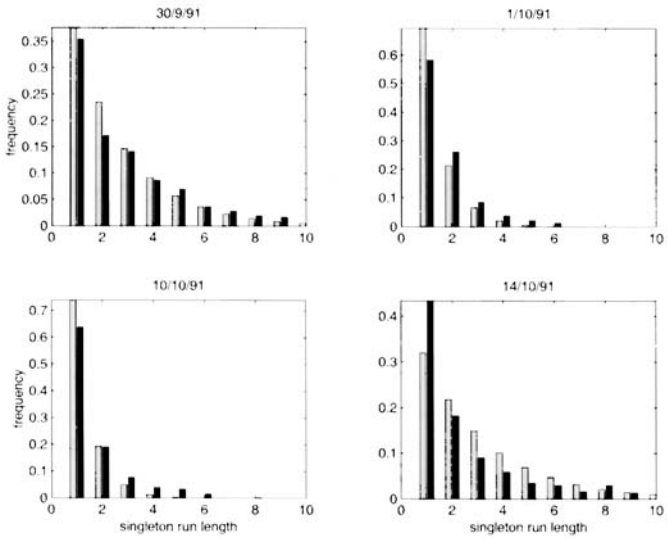

Fig. 11. Histogram of the lengths of unbroken sequences of single dot profiles (dark bars) alongside the expected frequency (light bars) for the four study days. Agreement is good, except for 14 October 1991, the day with greatest dots per profile. This implies that each detected dot is a separate entity, and remains in the acoustic beam for less than the profile repetition time.

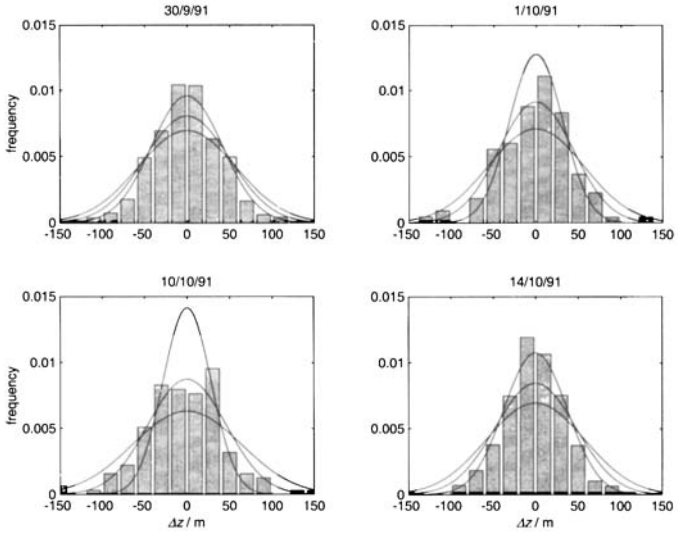

Fig. 12. Histograms of Δz, the change in target height between sequential dots. Overlaid in each case are the expected forms of the histogram for a random population, assuming a Gaussian scatter about some mean height. The curves are for the mean Gaussian scatter, $<\sigma z_i>$ and the upper and lower confidence limits in $<\sigma z_i>$ given by $\sigma(\sigma z_i)$ (see Table I). The agreement is reasonable, implying that the recorded height of each target is not related to the height of previous target.

The lack of target persistence is confirmed by analysis of the target height distribution. Figure 12 shows histograms of Δz, the change in height from one profile to the next for continuous runs of single target profiles. Overlaid on Fig. 12 is the expected distribution, using the corresponding local dot echo layer depth, $<\sigma z_i> \pm \sigma(\sigma z_i)$, taken from Table I. Persistent targets with a small vertical velocity would enhance the histogram at $\Delta z \approx 0$. The agreement of the histogram distributions with the expected curves again confirms the lack of persistence in the dot echo targets.

Each detected target is apparently a separate entity; hence they are either short lived, or are travelling at a horizontal velocity which ensures that they are within the acoustic beam for less than 10 seconds. An estimate of the lower limit of this velocity, v_{min}, is given by

https://doi.org/10.1017/S0954102002000755 Published online by Cambridge University Press

Table II. Local surface meteorology for the four case study days. The westerly wind direction observed on these days may be significant, as easterly winds prevail at the site. Cloud cover is minimal or thin, and for the first three case studies, the surface was cooling rapidly. Wind speeds were lighter than average.

Date & time	U/ms^{-1}	wind direction/°	T/°C	low cloud cover/octas
30/09/91 18:00	2.5	270	-23.7	7 (As)
21:00	2.5	270	-25.3	6 (As)
01/10/91 18:00	5.0	240	-23.9	1 (Sc)
21:00	5.5	250	-28.4	1 (Sc)
10/10/91 18:00	4.5	250	-24.8	1 (As)
21:00	5.0	250	-29.1	0
14:10/91 18:00	3.0	270	-22.4	1 (Sc)
21:00	2.5	260	-22.2	1 (Sc)

$$v_{\min} \approx \frac{\sqrt{A}}{10} \tag{5}$$

where A is the cross sectional area of the beam at the given range. From the beam width calculations above v_{min} is in the range of 8 to 14 ms^{-1}.

The local surface meteorological conditions for the four case studies are presented in Table II. The only significant correlation between the echo signature climatology and the meteorological data is in wind direction. Halley experiences predominantly easterly winds whilst the Sodar data selection criteria coincide with less frequent westerly surface winds. At the site, such conditions correlate with south-westerly winds aloft (King 1989).

Discussion

Dot echoes in Sodar echogrammes previously observed in non-polar latitudes have been identified with biological targets (Cronenwett *et al.* 1972). Mastrantonio *et al.* (1999) give a review of the relevant literature for both acoustic radars and similar effects for standard radar, which are now used for the tracking of insect swarms and bird migration.

The identification of the target observed at Halley as biological is still not proven, and the data to date are circumstantial. Possible atmospheric mechanisms for dot echo detection have been proposed, such as small scale temperature and humidity fluctuations (Mingyu *et al.* 1981), water vapour fluctuations (Singal *et al.* 1985), or a condensation/evaporation mechanism (Rao *et al.* 1995), but in all these cases, there is no corroborative evidence, either *for* an atmospheric mechanism, or *against* a biological source. It is still possible that all dot echo targets observed to date are due to birds, bats or insects.

The Halley dot echo data, when first presented (Anderson 1996) appeared to be a confounding case, as there was both an unlikelihood of a moisture signature in the backscatter and the belief that there were no birds in the area in any significant numbers. The atmospheric mechanisms suggested by Mingyu *et al.* 1981, Singal *et al.* 1985 and Rao *et al.* 1995 all depend on the presence of moisture to produce an additional scattering effect. The cold temperatures of the atmosphere in polar regions reduces the available absolute humidity to low values compared to lower latitude sites. Moreover, Sodars operating at two other Antarctic coastal sites, viz Terra Nova Bay and Dumont d'Urville, under similar conditions to those at Halley have not recorded dot echo signature (Argentini *et al.* 1996 and Argentini, personal communication 1998 respectively).

A physical explanation for the dot echo phenomena requires both a micro-mechanism for the individual scatterers (each dot) and an additional macro-mechanism for the non-random distribution of the targets. Atmospheric phenomena can have large-scale structure that is non-random, generated by waves or a relaxation process. Such processes are legion; internal gravity waves within the atmosphere can produce banded clouds or periodic clear air turbulence. Relaxation processes produce cloud streets, or vortex (rotor) shedding. An observation of a non-random distribution of targets is not sole proof, *per se*, of a biological as opposed to physical generation mechanism, but it does limit the number of plausible physical mechanisms to those which must be sensitive to a larger scale wave-like process.

Observations that there are birds colonies to the south of Halley whilst there are no known colonies south of either Terra Nova Bay and Dumont d'Urville (van Franeker 1999) are again only supportive of the biological case.

The velocity estimates of 8–14 ms^{-1} are qualitatively consistent with the targets being smallish birds. Alerstam *et al.* (1993) present radar tracking measurements of flight speeds for a range of seabirds, and compare them to theoretical estimates of different forms of flight, as given by Pennycuick (1989). Although the Antarctic petrel is not included in these measurements, the study indicates that seabird flight velocity falls somewhere between the optimum for gliding (maximum range for a given height loss) and optimum for flapping (minimum energy expenditure for a given range). These measurements were for birds over water, where large birds especially, can gain energy from "swell soaring". For these Sodar targets, swell soaring is obviously not possible, and the velocity might be biased towards the flapping flight optimum. At least two major unknowns will affect such flight velocity: the mean ascent/descent rate, and the main air velocity at the height. Neither is known, although the low westerly surface wind speeds at this site (as given in Table II) are usually associated with low wind speeds aloft. Notwithstanding these uncertainties, if an Antarctic petrel is assumed to be flapping, with negligible vertical velocity (sink or climb) and is somewhere between a Wilson's petrel and a little shearwater (to be able to use Alerstam *et al.*'s measurements) then its velocity should be between 9 and 12 ms^{-1}.

The sink or climb question is pertinent: a serious concern that hovers over these data is that layered dot echo signature has not been observed in recent years at Halley, despite the redeployment of a similar acoustic radar at the station. During

https://doi.org/10.1017/S0954102002000755 Published online by Cambridge University Press

1998 to 2000, a modified acoustic sounder has recorded echo signature up to 1000 m, again primarily for turbulent boundary layer studies, and analysis of these data indicate that dot echoes are still apparent, but at much lower density and unlike the 1991 data, with no preferred altitude. The present acoustic system is semi-autonomous, and has a lower sensitivity, but dot echoes are still detected. Perhaps the more significant difference is that the present system is running at Halley V, which replaced Halley IV in 1992. The new station, built to the east of Halley IV, was in 1998 some 8 km further east of the site of Halley IV in 1991, and this may explain the absence of the dot layer signature. Halley is built on a floating ice shelf which is drifting and spreading north and west; the coastline is relatively constant (due to calving) so the station (both IV and V), situated on a ice flow lines running almost due west, effectively creep towards Precious Bay over time. The two data sets are thus not necessarily comparable if there is a large horizontal variability in the target density, or if the target layer altitude is sensitive to position. This is plausible for bird targets, given the history of observations of birds at the series of Halley stations from 1957.

As the dot echo data stand, there are two further counter-arguments for the signature being for birds. Firstly, and most simply, there were no corroborative observations of flocks of birds over-flying Halley IV when the acoustic data were recorded. Secondly, the dot echo density is large when compared to subsequent observations of Antarctic petrels nesting in the Theron Mountains. The case against is less well held given some historical data of bird observations at the site.

Lack of direct observation of the assumedly large numbers of birds flying over a permanently occupied station such as Halley IV is explained by the fact that at 700 m altitude, a typical Antarctic bird such as a petrel is barely detectable by the naked eye. Assuming a target size of 10 cm, the angular resolution needed to see such a target at 700 m is equivalent to seeing a dot of size 0.1 mm at arms length, about 20 times smaller in area than this full stop. The targets generally seen by the Sodar are in single numbers in a beam cross section of at least 6000 m^2. With the same scaling to arms length, 6000 m^2 at 700 m is equivalent to a piece of A5 paper. Note also that, except for the skua, from underneath, all flying Antarctic species are light in colour, and would therefore not show a marked contrast against cloud or clear sky. Also note that these estimates are for looking directly up, which few people tend to do, and at any angle away from the vertical, the distances to the targets are even greater. It is therefore entirely plausible that the birds are there but have not been seen.

The second counter argument is that the target density observed by the Sodar is too large to be supported by such a small biomass as observed thus far, that is, the estimate of 40 000 or so pairs seen in the Theron Mountains. With roughly one target every 6000 m^2 (assuming d_{pp} of near unity), in a near continual coverage over 24 hours, and assuming these creatures are travelling to and from the nesting sites some 350 km away, then the trail swath would be of the order of 1 km. This is the narrowest limit; the d_{pp} is often less than unity, and the beam cross section could be some two times wider, and the Theron pair estimate might be low, but even a 100 km wide swath implies that the birds are flying preferentially towards the Brunt Ice Shelf and not in any other direction; a 100 km swath at Halley subtends a 16° angle at the Therons. Note from Fig. 1 that the edge of the continent is actually much closer to the mountains further west. With a horizontal target velocity estimate of around 10 ms^{-1}, the trip to and from the Therons would take about 20 hours.

Initially, this would appear to be a strong case against birds being the target, as a secondary case must now be made for the Brunt Ice Shelf area being in some way special or unique. Although there is a danger in singular *ad hoc* explanations, the Halley environs may well be significant to foraging birds because of the perennial presence of coast open water on the west ice shelf coast. The Precious Bay area, 14 km to the west of Halley IV in 1991, (22 km west of Halley V in 1998) is known to be free of sea ice, even in winter, (Anderson 1993), and would therefore provide access to food throughout the observations, especially when other areas were covered in sea ice. Preferential use of coastal open water (polynyas) by foraging birds has been confirmed by satellite tracking of Antarctic petrels in Dronning Maud Land, and hence making a special case for the Brunt Ice Shelf area is not so tenuous (J. Croxall personal communication 2001).

The Precious Bay polynya foraging hypothesis, if correct, implies that there will be a sink / climb rate between the observed echo altitude at Halley IV (14 km from the polynya) and sea level at the polynya. Assuming the simplest direct line of flight, the sink/climb angle will be around 3 degrees (700 m in 14 km). Note that this is on the most "favourable" days, when the layer was completely resolved in the vertical, and often the dot echo layer was around 1000 m, giving a sink/climb angle of 4 degrees. Moreover, at the present station position, (22 km from the coast) at the same sink/climb angle, the birds will be at 1.1 km altitude, that is above the height of the Sodar range.

The meteorological climatology shows an indication that the targets are observed more clearly and at a lower altitude during days when the surface winds were from the less frequently observed westerly direction. Could it be that the birds arrive at the station more quickly (and hence at a lower altitude) when the wind is in their favour?

Further supporting for evidence for a Precious Bay flight path over the Brunt Ice Shelf can be implied from observations of Antarctic petrels at previous sites of the Halley station. Brook & Beck (1972) present estimates of Antarctic petrels nesting in the Theron Mountains from a visit in 1966/67 and 1967/68, and also including direct observations of the birds over Halley Bay (effectively Halley II) by M. Thurston made in 1960 (BAS internal report). Two aspects of Thurston's observations are noteworthy. Firstly that the birds were seen, and in significant numbers, and most intriguingly, all but one of the observations have the birds flying south-west. That the

birds were seen at Halley II (75°30'S, 26°40'W, 1960) fits with the above flight path scenario, as the base was only four to five kilometres from the coast, either to the east or north. Given the estimated flight path s/c angle above, the birds would be at around 225 m, but Thurston's report gives the observed altitude at the base as typically 50–100 ft (15–30 m), apparently using the base masts as migration markers.

Following this line of discussion, if the observed Halley II Antarctic petrels were indeed flying back to the Therons (and very rarely *from* the Therons), it is apparent that they use a circular foraging path, with the southern going leg overflying the Halley II base position, and then presumably the future Halley IV_{1991} position, almost due south of Halley II_{1960}. Such a circular route would be advantageous given an understanding of the climatology of katabatic and barrier wind flow in the region:

- Local wind profile climatology indicates that at the start of October at Halley IV, there was a mean northerly component of the wind, with a maximum at around 700 m. (King 1989)
- Models of large scale drainage flows (katabatics) indicate that the flow rate is greatest where there is greatest slope, and where there is a significant upstream catchment area for cold air (Parish & Bromwich 1987)
- Recent mesoscale modelling of katabatic flow from an ice sheet onto an ice shelf show that the flow tends to be blocked from the ice shelf (Renfrew & Anderson in press).

From a wind flow perspective, the best round route to Precious Bay from the Theron Mountains is therefore to head west down the basin between the Therons and Touchdown Hills, north along the coast to Precious Bay, and then south to south-west, back over the Brunt Ice Shelf and up onto the continental plateau via Coats Land. The last part of this route involves travelling up an incline with no upslope catchment area, and no local flow convergence, thereby giving the weakest overall katabatic headwind for a given gain in altitude. It might be of interest to quantitatively model the foraging energy expenditure for a range of paths assuming the none-conserved assistance/hindrance from the katabatic wind regime which might offset the distance added to the direct line of flight route.

Conclusions

The climatology of the dot echo signature observed at the Halley station bears many resemblances to confirmed echoes from bats or birds, but there are a number of remaining doubts as to the exact nature of these data. Birds have not been observed in such large numbers over the base, although the density (one every 70 m or so) and the altitude (700+ m overhead) ensure that they would barely detectable by the naked eye. The source of the birds would have to be on rocky outcrops, of which the closest is a few hundred kilometres away, and the data imply that they must fly to Halley preferentially for their number density to be large at the observing site. This claim is to some extent validated by the known perennial open water at the western coast of the ice shelf. The statistical analysis of target distribution gives pause to claims of a physical mechanism, such as a turbulent or meteoric effect. Lack of direct bird observations in 1991 and even acoustic observations since 1998 can then be explained by a circular foraging route between the assumed breeding area in the Theron Mountains to perennial open water off the Brunt Ice Shelf, with a 3° ascent rate after leaving the open water at the coast. Such a route might be energetically advantageous to the birds, given the variable katabatic wind regime in the area.

Acknowledgements

I thank John King, John Croxall, Igor Petenko and Giangiuseppe Mastrantonio for encouragement and much helpful advice during the course of this work. I also thank Stefania Argentini and Alcide di Sarra for many helpful comments during the review processes.

References

Alerstam, T., Gudmundsson, G.A. & Larsson, B. 1993. Flight tracks and speeds of Antarctic and Atlantic seabirds: radar and optical measurements. *Philosophical Transactions of the Royal Society, London*, **B340**, 55–67.

Anderson, P.S. 1993. Evidence for an Antarctic winter coastal polynya. *Antarctic Science*, **5**, 221–226.

Anderson, P.S. 1996. Comparison of internal gravity waves events recorded by Sodar and microbarograph over an Antarctic ice shelf. *In* Kallistratova, M.A., *ed. Moscow ISARS '96: Proceedings.* Moscow: A.M. Obukhov Institute of Atmospheric Physics, 7.7–7.11.

Argentini, S., Mastrantonio, G., Viola, A., Pettré, P. & Dargaud, G. 1996. Sodar performance and preliminary results after one year measurements at Adélie and coast, east Antarctica. *Boundary-Layer Meteorology*, **81**, 75–103.

Brook, D. & Beck, J.R. 1972. Antarctic petrels, snow petrels and South Polar skuas breeding in the Theron Mountains. *British Antarctic Science Bulletin*, No. 27, 131–137.

Cronenwett, T.W., Walker, G.B. & Inman, R.L. 1972. Acoustic sounding of meteorological phenomena in the planetary boundary layer. *Journal of Applied Meteorology*, **11**, 1351–1358.

Croxall, J.P., Steele, W.K., McInnes, S.J. & Prince, P.A. 1995. Breeding distribution of the snow petrel *Pagodroma nivea*. *Marine Ornithology*, **23**, 69–99.

King, J.C. 1989. Low-level wind profiles at an Antarctic coastal station. *Antarctic Science*, **1**, 169–178.

Mastrantonio, G., Naithani, J., Anderson, P.S., Argentini, S. & Petenko, I. 1999. Quantitative analysis and interpretation of dot echoes observed with a Doppler Sodar. *Journal of Atmospheric and Oceanic Technology*, **16**, 1928–1940.

Mingyu, Z., Naiping, L., Yanjaun, C. & Shiming, L. 1981. The lump structure of turbulent field in atmospheric boundary layer. *Scientia Sinica*, **24**, 1705–1716.

Parish, T.R. & Bromwich, D.H. 1987. The surface windfield over the Antarctic ice sheets. *Nature*, 328, 51–54.

PENNYCUICK, C.J. 1989. *Bird flight performance: a practical calculation manual.* Oxford: Oxford University Press, 153 pp.

PETENKO, I.V. & KALLISTRATOVA, M.A. 1996. Dash echo structure as observed by acoustic sounding. *In* KALLISTRATOVA, M.A., *ed. Moscow ISARS '96: Proceedings.* Moscow: A.M. Obukhov Institute of Atmospheric Physics, 6.109–6.114.

RAO, M.P., CASADIO, S., FIOCCO, G., LENA, F., CACCIANI, M., CALISSE, P.G., DI SARRA, A. & FUA, D. 1995. Observation of lump structures in the nocturnal atmospheric boundary layer with Doppler Sodar and Raman lidar. *Geophysical Research Letters*, **22**, 2505–2508.

RENFREW, I.A. & ANDERSON, P.S. In press. The surface climatology of an ordinary katabatic wind regime in Coats Land, Antarctica. *Tellus.*

SINGAL, S.P., GERA, B.S. & AGGARWAL, S.K. 1985. Studies of Sodar observed dot echo structures. *Atmosphere-Ocean*, **23**, 304–312.

THURSTON, M.H. 1960. Ornithological Report, 1960. *BAS Archives, AD6/2Z/1960/Q1* [Unpublished]

van FRANEKER, J.A., GAVRILO, M., MEHLUM, F., VEIT, R.R. & WOEHLER, E.J. 1999. Distribution and abundance of the Antarctic petrel. *Waterbirds*, **22**, 14–28